The University of Queensland
Australia

gciQ Global Change Institute

Comparative Productive Performance of Three Solar PV Technologies Installed at UQ Gatton Campus

Oct 2016
DISCUSSION PAPER #3

Prepared by Phillip Wild, PhD
Postdoctoral Research Fellow
Global Change Institute
The University of Queensland

Comparative Productive Performance of Three Solar PV Technologies Installed at UQ Gatton Campus

By Phillip Wild
Email: p.wild@uq.edu.au
Telephone: work (07) 3346 1004; Mobile 0412 443 523

Version 4 – 12 Oct 2016

Abstract

Economic assessment of the viability of different types of solar PV tracking technologies centres on assessment of whether the annual production of the different tracking technologies is increased enough relative to a benchmark Fixed Tilt system to compensate for the higher installation and operational costs incurred by the tracking systems. To investigate this issue, we use the PVsyst software to simulate electricity production from three representative solar PV systems installed at Gatton. In these simulations we use hourly solar irradiance, weather and surface albedo data, technical data relating to both module and inverter characteristics and impacts associated with module soiling and shading. A key finding was that over the period 2007 to 2015, average increases in simulated annual production of between 17.7 and 17.9 per cent and 36.5 and 36.7 per cent were obtained for Single-Axis and Dual-Axis tracking systems relative to the Fixed Tilt system.

(1) Introduction

The economics of solar PV has changed significantly over the last decade with installation costs declining significantly following the marked take-up of solar PV systems, often on the back of generous Government feed-in tariff support particularly in Europe. More recently, a marked increase in the up-take of roof-top solar PV occurred in Australia on the back of generous state-based feed-in tariffs schemes and the Federal Government's small-scale renewable energy target (RMI, 2014). Unlike the case in particularly Spain and

Germany, however, there were no equivalent feed-in tariffs available for large-scale investments in Australia, and these types of investments have been much slower to emerge.

To-date, investment in utility scale solar PV projects has largely proceeded on the basis of support from two particular programs: (1) Australian Capital Territory (ACT) reverse auction for solar PV projects (ACT, 2016); and (2) Government support from the Australian Renewable Energy Agency (ARENA, 2016), in conjunction with financial support from the Clean Energy Finance Corporation (CEFC) for larger projects (CEFC, 2016). This has occurred against a general backdrop of a concerted attack on Renewable Energy in Australia since late 2013. Moreover, policy and regulatory uncertainty accompanying this attack has led to a general drying up of investment in large-scale renewable energy projects with major retail electricity companies now appearing unwilling to enter Power Purchase Agreements (PPA) traditionally needed to secure private sector finance for projects. This has led to the situation whereby the required capacity to meet the 2017 Large-scale Renewable Energy Target (LRET) now appears to be between 3000 and 4400 MW's in arrears (Green Energy Markets, 2015, 2016).

The structure of this paper is as follows. The next section will give a brief description of the solar array at the UQ Gatton Campus that underpins the modelling performed for this paper. Section (3) will contain a discussion of critical aspects affecting the comparative assessment of the production of representative technologies contained in the solar array under investigation. This will include an outline of the modelling employed in the paper to calculate solar PV yield and discussion of the results of the modelling relating to production and annual capacity factor (ACF) outcomes, respectively. Section 4 will contain conclusions.

(2) University of Queensland Gatton Solar Research Facility (GSRF)

The GSRF was funded under the Federal Government's Education Investment Fund (EIF) scheme ($40.7M), and was part of the larger ARENA funded project Australian Gas and Light Pty Ltd (AGL) Nyngan and Broken Hill Solar Farms (UQ, 2015a). These two solar PV farms have a capacity of 102 MW and 53 MW, respectively. The total cost of the combined project was $439.08 million, of which ARENA contributed $166.7 million and the New South Wales State Government $64.9 million (AGL, 2015). The objective of the EIF Project was to act as a pilot for the utility-scale plants – proofing technology and establishing supply chains.

The GSRF solar array installed at Gatton is a 3.275 megawatt pilot plant that comprises three different solar array technologies: (1) a Fixed Tilt (FT) array comprising three identical 630 kW systems (UQ, 2015b); (2) a 630 kW Horizontal Single Axis Tracking (SAT) Array utilising First Solar's SAT system (UQ, 2015c); and (3) a 630 kW Dual Axis Tracker (DAT) utilising the Degertraker 5000 HD system (UQ, 2015d). A good overview of the principals underpinning sun-tracking methods can be found in Mousazadeh et al. (2009).

An overhead picture of the Gatton array is contained in Figure 1. The FT system design at Gatton has the following technical design features: (1) all modules have a tilt angle of 20 degrees; (2) all modules have an azimuth angle of 357 degrees (e.g. modules are facing in the direction of three degrees west of north). The three FT arrays have a combined total of 21, 600 modules. These arrays can be located, respectively, at the top right hand side (termed the 'top' FT array) and with the main FT array being located just below the buildings and line of trees but above the road in Figure 1.

The SAT array has the following technical aspects: (1) the array is a horizontal array and thus has a tilt angle of 0 degrees; (2) the array has an azimuth angle of 357 degrees (e.g. same as the FT system); (3) maximum tracker rotation limit is set to 45 degrees; and (4) no backtracking is implemented. Backtracking is a control procedure that is used in some SAT systems to minimise the degree of self-shading from nearby SAT trackers. The total number of modules in the SAT array is 7,200 modules with 120 individual SAT tracking systems. The SAT array can be located in Figure 1 immediately below the top FT array, adjacent to the main FT array and also above the road in Figure 1.

The third array is the DAT array. There are 160 individual trackers installed at Gatton that are capable of a 340 degree slewing motion and a 180 degree tilt that allow the panels to directly face the sun at all times of the day, thereby maximising output (UQ 2015d). As in the case of the SAT system, the DAT system also has 7,200 modules in total. In Figure 1, the DAT array is located underneath the main FT array and below the road.

Figure 1. Overhead Picture of the UQ Gatton Solar Array

The same type of modules are installed on all three solar array technologies located at GSRF – First Solar FS-395 PLUS (95 W) modules. The same type of inverter is also installed with each of the 630 kW systems – SMA Sunny Central 720CP XT inverters. The three FT sub-arrays are connected to three inverters while the SAT and DAT arrays are connected to a single inverter each. Hence, the whole array contains five inverters. Moreover, through the connection agreement with the local Distribution Network Service Provider Energex, each inverter's output is limited to 630 kW.

In this paper we restrict attention to a comparative assessment of the production results of three representative 630 kW FT, SAT and DAT arrays. This will involve assessing the output performance of the SAT and DAT arrays and the left hand side sub-array of the main FT array installed at Gatton – e.g. the left most FT array looking at Figure 1.

(3) Comparative Assessment of Production Outcomes of the Three Representative Arrays.

Economic assessment of the viability of different types of solar PV tracking technologies typically centres on assessment of whether the annual production of the different tracking technologies is lifted enough relative to a benchmark FT system in order to compensate for the higher cost of installation and operational expenditures incurred by the tracking systems. The installation costs refer to the 'overnight' ($/Wp) or equivalently

($/kW) installation costs that would be incurred if the whole solar PV plant could be constructed overnight. This expenditure category would include costs associated with the purchase of modules and inverters as well as various categories of balance of plant costs. The latter component would include expenditures associated with: (1) costs of transport to site; (2) site preparation, racking and mounting activities; (3) DC and AC electrical connection; and (4) other non-production activity such as insurance costs, administration and connection licensing (RMI, 2014).

The second cost component is operational costs, in particular, Operational and Maintenance (O&M) expenditures associated with keeping modules and inverters operating efficiently. For tracking systems, additional O&M costs would also have to be levied against the need to also keep the tracking infrastructure working efficiently. In general, solar tracking systems include a tracking device, tracking algorithm, control unit, positioning system, driving mechanism and sensing devices (Mousazadeh et al, 2009).

Large optical errors in tracking the sun's position will result in potentially large reductions in electricity generated from the PV system relative to what would have been obtained if the tracking mechanism was working properly. A crucial question, however, is how large is how large? Mousazadeh et al. (2009) point out that trackers do not need to be pointed directly at the sun to be effective. They argued that if the aim is off by 10 degrees implying an optical tracking error of 10 degrees, the output will still be 98.5% of the full-tracking maximum. Stafford et al. (2009) report that tracking errors may not be negligible when compared with typical system acceptance angles – the maximum pointing error that the PV system can tolerate without a substantial loss of power output. They also found that the fraction of available energy captured tended to decline with the degree of the system's acceptance angle, whilst increasing with the degree of the acceptance angle. Additional support for this broad finding is also cited in (Sallaberry et al, 2015a, p. 195). However, complicating this issue is the observation in Stafford et al (2009) that different solar technologies such as High Concentration Photovoltaic (HCPV), Low Concentration Photovoltaic (LCPV), Concentrated Solar Thermal (CSP) and single- and dual-axis tracked flat-plate PV panels all have different relationships between generated power and tracking error, leading to different tracking requirements for each technology.

If large reductions in output arise because of the presence of large optical tracking errors relative to the system's acceptance angle, this would impair the economic viability of the tracking system. Some electricity must also be consumed internally by the system in order to operate the motors that drive the shifts in position of one or more of the axes associated with the particular tracking mechanism. This internal electricity consumption is typically netted of the gross output produced by the system when tracking is operating during the day.

Thus, O&M expenses are likely to be directly proportional to the complexity of the tracking system employed. As such, O&M provisions associated with more complex two axis trackers such as the DAT system are likely to be of a higher magnitude because the tracking infrastructure is more complex and larger in scale and is, therefore, more likely to be prone to mechanical faults or break-downs.

(3.1) PV Yield Assessment Using PVsyst

The PVsyst software (PVsyst, 2016a) was used to simulate electricity production of the three representative solar PV systems installed at GSRF. To run simulations in PVsyst, various user supplied inputs are required. These relate to: (1) hourly solar and weather data; (2) technical information about modules, inverters and array sizing and design; (3) soiling effects; (4) shading effects; and (5) DC and AC electrical losses. In the modelling performed for this paper, we also assumed that all modules, inverters and tracking infrastructure were in good working order.

(3.1.1) Solar and weather data

The solar and weather data are stored in special 'Meteo' databases produced by PVsyst from user-supplied solar irradiance and weather data as well as information on the solar PV site's latitude, longitude, elevation and time zone (Mermoud and B. Wittmer, 2014, Part 3). The solar data included Global Horizontal Irradiance (GHI) and Direct Normal Irradiance (DNI) data. Diffuse Horizontal Irradiance (DHI) data is calculated by PVsyst using internal calculations of the sun's position by the software given the latitude, longitude, elevation of the site and commencing date and time of the simulation. The Perez Sky Diffuse model is used to determine Plane-of-Array (POA) irradiance (PVsyst, 2016f)[1].

The GHI and DNI data were obtained from the Australian Bureau of Meteorology's (BOM) hourly solar irradiance gridded data (BOM, 2015). The climate data required by

[1] Specific information about this transpositional model can be found in PVsyst help (PVsyst, 2016f) by following the following path: 'Physical models used/ Irradiation models/ Transposition model'.

PVsyst include ambient temperature (degrees Celsius) and wind speed (metres per second). This data was sourced from the BOM's Automatic Weather Station (AWS) located at the University of Queensland Campus at Gatton.

We also calculated surface albedo data for input into PVsyst. This surface albedo data was compiled from MODIS White Sky Albedo data (NASA, 2015). This was taken from representative two weekly samples taken at the Gatton latitude and longitude coordinates to reflect differences in both season and ENSO cycle status. Specifically, averages of MODIS white albedo readings were obtained for the list of dates in Table 1. The surface albedo values used in the simulation by year and month are listed in Appendix A, Panel (A).

Table1. Dates used to Estimate Surface Albedo by Season and ENSO Status

Season	La Nina	ENSO Neutral	El Nino
Summer	9-24 January 2009	11-26 December 2013	10-26 December 2009
Autumn	7-22 April 2010	7-22 April 2013	7-22 April 2006
Winter	2-17 June 2010	10-25 June 2013	10-25 June 2006
Spring	8-23 October 2010	16-31 October 2013	16-31 October 2009

(3.1.2) Module, inverter and solar array design

Data is also required about the technical characteristics of the modules and inverters used at GSRF. As mentioned above, the modules used are First Solar FS-395 PLUS (95 W) modules while the inverters are SMA Sunny Central 720CP XT inverters. In PVsyst, technical information on modules and inverters are typically supplied by their manufacturers in the form of '.PAN' files for modules and '.ONP' files for inverters. These files are incorporated as part of the large internal product database included in the PVsyst software. Both the First Solar module type and SMA inverter type mentioned above were included in this internal database and subsequently selected within the PVsyst modelling environment.

Recall that for each of the three FT, SAT and DAT systems modelled, 7200 modules and a single inverter was used, with the inverter's AC output constrained to 630 kW in each case.

Typically, PV performance is defined relative to Standard Testing Conditions (STC). This includes a temperature of 25 degrees Celsius. However, PV module performance will decrease with increases in temperature. The loss is based on the module's power temperature coefficient and a field thermal loss factor. The thermal loss factor is the rate of module heat loss and can be attributed to the effects of convection. First Solar has proposed a thermal loss factor of 30.7 W/m2 for "free" mounted modules with air circulation (ARUP, 2015). This value was adopted in the PVsyst simulation modelling.

The reflection loss is based on specific information provided by First Solar. Reflection losses are associated with the incidence angle at which the sun is entering the atmosphere and striking the surface of the module. At incidence angles which are not normal to the atmospheric layer or to the module there will be a certain degree of reflectance. This loss is based on an Incidence Angle Modifier (IAM) defined for various angles. In the PVsyst modelling the incident angle effect is calculated using the ASHRAE model with default value for the b_0 coefficient of 0.05 (ARUP, 2015).

Implementation of PVsyst modelling also required data relating to system design features. In the design and sizing of the array, the most crucial information is: (1) number of modules in a string; (2) number of strings in parallel; and (3) number of inverters. From this information as well as from additional information relating to both modules and inverters, the following system information is determined: (1) maximum DC capacity of the solar array; and (2) maximum AC output capacity of the inverters. The key system design parameters and quantities used in the PVsyst simulations are reported in Panel (B) of Appendix A.

(3.1.3) Soiling effects

To run simulations in PVsyst, account needs to be taken of module soiling. It is generally accepted that after solar irradiance and air temperature, module soiling will be the next most crucial issue affecting solar PV yield. Four different soiling rate assumptions were employed in the modelling for the paper. These relate to low, medium and high soiling scenarios, and additionally, a soiling scenario based upon recommendations of First Solar (ARUP, 2015).

All soiling scenarios are based on consideration of recorded daily rainfall over the period 2007 to 2015. The rainfall data utilised in constructing the various soiling scenarios is that recorded at the UQ Gatton Campus BOM AWS located within two kilometres of the solar farm. The mean average monthly rainfall for this site is presented in Figure 2. This figure clearly shows a wet season encompassing the period November to March and a dry season arising over the period April to September with a transition period between these two regimes occurring in October.

In determining monthly soiling rates, it was assumed that 25 millimetres (mm) or more of rainfall during a particular day in a month would be sufficient to restore the modules to their 'pristine' condition associated with their commissioning. During the wet season, it was common to have some days with a couple of inches of rainfall and multiple days with over an inch of rainfall. Similarly, it was assumed that daily rainfall totals of less than 5 mm was not sufficient to engender any cleansing of the modules. Partial cleansing effects were assumed for daily rainfall totals between 5 mm and 25 mm.

Figure 2. Mean average rainfall at UQ Gatton Campus BOM AWS

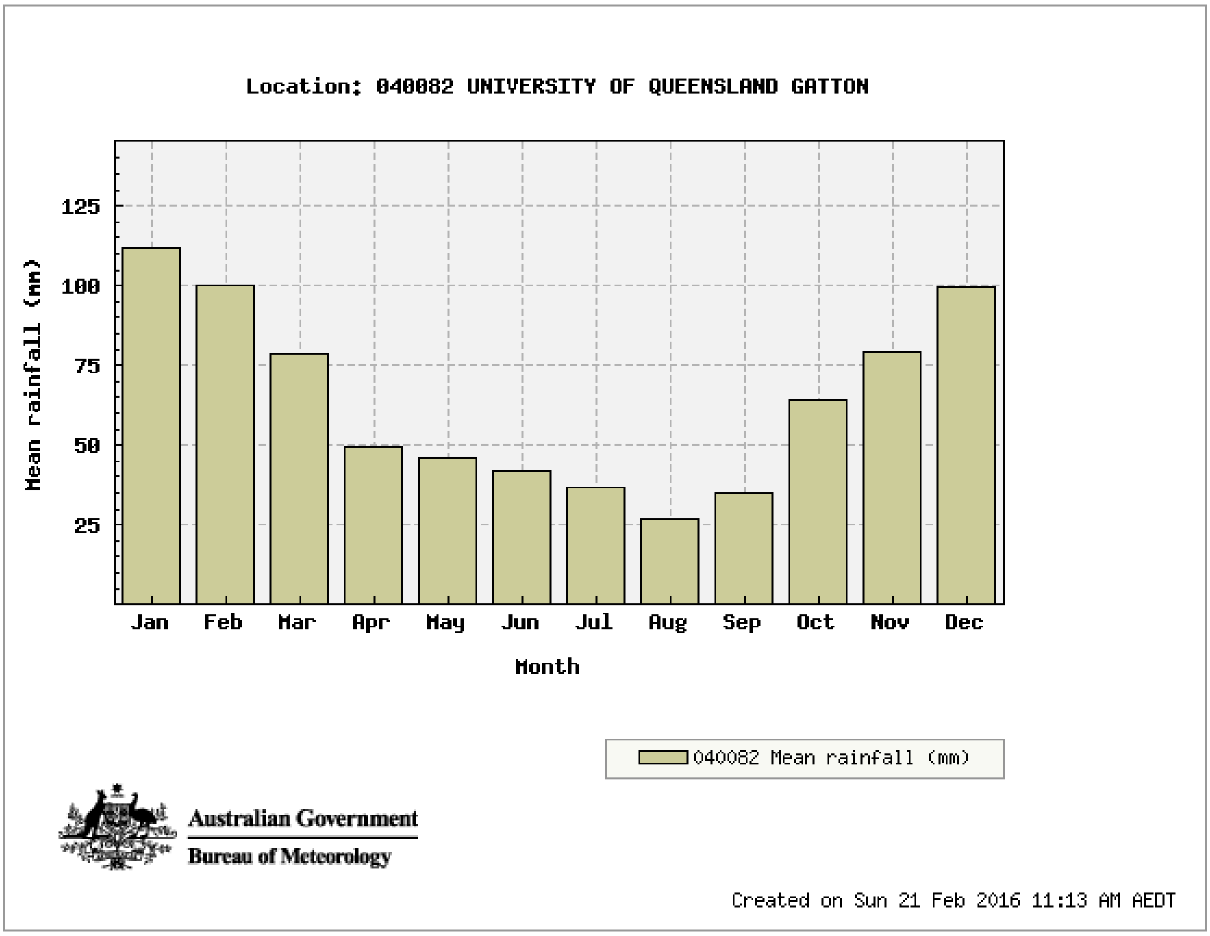

Accumulative soiling was calculated from the monthly rainfall totals recorded for the UQ Gatton Campus BOM AWS for two different daily soiling rates assumptions associated with daily rainfall totals within each month that was less than or equal to 5 mm. The low soiling scenario assumed a daily growth in soiling effect of 0.033% per day. The medium soiling scenario assumed a higher daily soiling rate of 0.11% per day, adopted from (Kimber et al, 2006) who estimated this daily soiling rate for rural areas in Central Valley and Northern California – for example, see Figure 3 of (Kimber et al, 2006). Assuming a 30 day month, these two daily soiling rates would produce monthly soiling rates of 1.0 and 3.3 per cent, respectively.

If daily rainfall exceeded 25 mm during the month, total module cleansing was assumed with the monthly soiling rate being set back to the assumed 'pristine' commissioning rate of 1.0 per cent. If one or more of the daily rainfall totals during the month was between 5 mm and 10 mm, 80 per cent of the assumed within month soiling rate was added on to the previous months soiling rate thus indicating some marginal cleansing effect on the modules. If one or more of the daily rainfall totals was between 10 mm and 16 mm, 50 per cent of the assumed within monthly soiling rate was added onto the previous months soiling rate, indicating some partial cleansing effect on the modules. If one or more of the daily rainfall totals fell between 17 mm and 25 mm, only 20 per cent of the assumed within monthly soiling rate was added onto the previous months soiling rate. Thus the main effect of daily rainfall between 5 and 25 mm is to offset some of the accumulated within month soiling effect with the larger impacts being associated with daily rainfall rates of between 17 mm and 25 mm.

For completeness, a fourth soiling scenario is also employed, based on an approach recommended by First Solar (ARUP, 2015, Section 4.2.1.3). This approach involves assuming a monthly soiling rate of 3.0 per cent if monthly rainfall was less than 20 mm, 2.0 per cent if monthly rainfall was between 20 mm and 50 mm and 1.0 per cent if the monthly rainfall was greater than 50 mm.

The monthly soiling rates were also corrected for local spectrum following the method advocated in First Solar (2015). This correction is based upon the fact that modules are rated under STC assuming a spectral distribution as defined by ASTM G173 for an air mass of 1.5. However, site-specific spectral irradiance will typically deviate from STC resulting in varying performance in regard to module nameplate capacity.

First Solar (2015) proposed a method to account for that type of difference based on a new variable termed a spectral shift factor, which was driven principally by the amount of precipitable water in the atmosphere. They proposed a method for estimating the amount of precipitable water in the atmosphere at a site's location from relative humidity and ambient temperature data recorded at the site. These hourly spectral shift factors are expressed as aggregate monthly spectral shift factors by first weighting the hourly factors by hourly solar irradiance (GHI) data and then averaging over each calendar month. These variables can be viewed as a relative loss or gain with respect to nominal energy with positive values depicting a loss in energy due to local spectrum whilst negative values denote an energy gain due to local spectrum.

In accordance with First Solar (2015), the monthly spectral shift factors are implemented by combining them with the monthly soiling loss factors to obtain an 'augmented' monthly soiling loss factor. In this context, a negative average monthly spectral loss factor (denoting energy gain) would reduce the original soiling loss factor. A positive average monthly spectral loss factor (denoting energy loss) would increase the original soiling loss factor.

The set of augmented monthly soiling loss factors for the four soiling scenarios considered are reported in Table 2. In calculating the augmented soiling losses, if the energy gain exceeded the original calculated soiling loss, the augmented soiling loss would become negative. In such cases, the absolute value of the smallest negative monthly augmented soiling loss was added to each average monthly augmented soiling loss factor to ensure that they were all non-negative. To offset this operation, this absolute value was similarly subtracted from one or more of the DC electrical loss factors to ensure a zero net change in loss factors. These subtractions were typically applied to DC mismatch and nameplate loss categories.

Table 2 indicates that the lowest augmented soiling losses occur during the 'Summer' wet season November to March reflecting both the additional cleansing power of higher rainfall totals as well as energy gains associated with local spectrum over these particular months. The values of zero in January point to this month containing the smallest negative augmented soiling factor losses originally, and whose absolute values were subsequently added to each monthly value to ensure that the augmented monthly soiling loss factors were all non-negative.

The 'Low', 'Medium' and 'First Solar' soiling scenarios were discussed above. The 'High' soiling scenario was calculated from the data derived under the medium soiling scenario that utilised a daily soiling growth rate of 0.11% per day. These values produced monthly values over each month for years 2007 to 2015. The Medium soiling scenario was calculated as the average of that data on a month-by-month basis. Similarly, the High soiling scenario was calculated as the 90th percentile of that data, on a month-by-month basis.

It is clear from Table 2 that the Low and First Solar soiling scenarios produce very similar results with annualised averages 1.7 and 1.8 per cent, respectively. The maximum soiling rates occur in the July to September time period in the range of 3.2 to 3.8 per cent whilst the lowest soiling rates occur in the December to March time frame in the range of 0.0 to 0.3 and 0.0 to 0.7 per cent, respectively. Because of this observed closeness, we will only report the results associated with the 'Low' soiling scenario as the generic low soiling scenario to be considered further in the paper.

In the case of the Medium soiling scenario, an annualised average of 3.2 per cent was obtained. Once again, the maximum and minimum soiling rates appear in the July to September and December to March time periods in the range of 6.6 to 7.0 per cent and 0.0 to 0.5 per cent, respectively. The results associated with the High soiling scenario denote more significant increases in both maximum and minimum soiling rates under this scenario although the periods when these rates arise continues to remain the same. Specifically, the maximum monthly augmented soiling rates are now in the range of 9.5 to 12.5 per cent while the minimum rates are in the range of 0.0 to 1.8 per cent. The annualised average for this particular scenario is 5.7 per cent.

Table2. Augmented soiling rate configurations (Percentage)

Month	Low	Medium	High	First Solar Rates
Jan	0.0	0.0	0.0	0.0
Feb	0.1	0.5	1.8	0.4
Mar	0.3	0.5	1.1	0.7
Apr	1.2	2.0	4.3	1.5
May	2.3	4.4	8.2	2.6
Jun	2.4	4.0	6.7	2.7
Jul	3.6	7.0	9.5	3.8
Aug	3.7	6.8	10.6	3.5
Sep	3.2	6.6	12.5	3.2
Oct	2.5	5.2	10.5	2.3
Nov	0.9	1.4	2.5	0.9
Dec	0.3	0.4	0.9	0.3
Annualised Average	1.7	3.2	5.7	1.8

(3.1.4) Shading effects

Solar PV yield assessment using PVsyst also requires that the effects of shading on modules in the PV field be accounted for. In PVsyst, three types of shading effects are accommodated. These are: (1) horizon shading; (2) near-object shading; and (3) self-shading.

Horizon shading deals with the shadings effects of objects sufficiently far away to act on the PV field in a global way. Specifically, at a given instant, the sun is either visible or not visible on the PV field. The distance of horizon shading objects is generally viewed as being at least ten times the PV field size (PVsyst, 2016b). Horizon shading impacts are not considered in this paper.

Near-object shading can be interpreted as a reduction in POA incident irradiation by external objects located near to the PV field such as buildings and trees. As such, near-object shading draws visible shades on the PV field. These shading effects are modelled as shading factors denoting the ratio of the shaded area to the total sensitive area of the PV field (PVsyst, 2016c).

Near-object shading affects direct (beam), diffuse and albedo POA irradiance. Analysis of near-object shading is performed in PVsyst using a three-dimensional shading perspective of each representative array and nearby external objects. Graphical representations of the three 3d shading perspectives of the three representative arrays are depicted in Figure 3, Panels (A)-(C). In these 3d shading perspectives, we employed a PVsyst 'PV sheds field' object to model the FT array and PVsyst 'PV tracking field' objects to model the SAT and DAT arrays as denoted in rows two and three of Table 3.

Figure 3. Graphical Depiction of 3d Shading Perspective of Each Representative Array

Panel (A). FT array

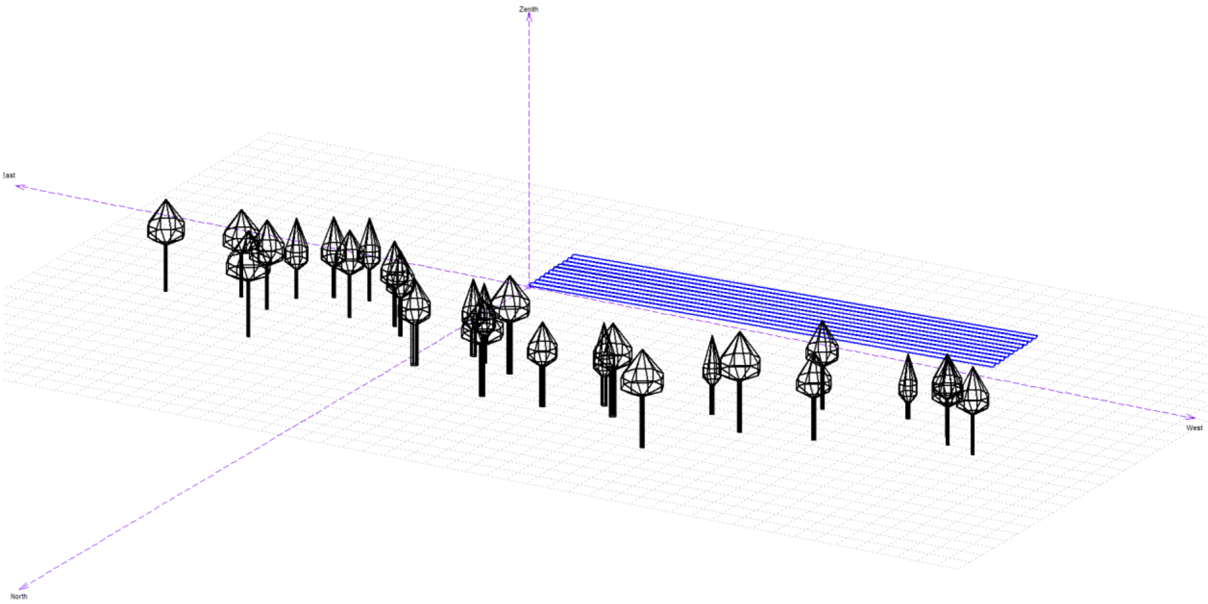

Panel (B). SAT array

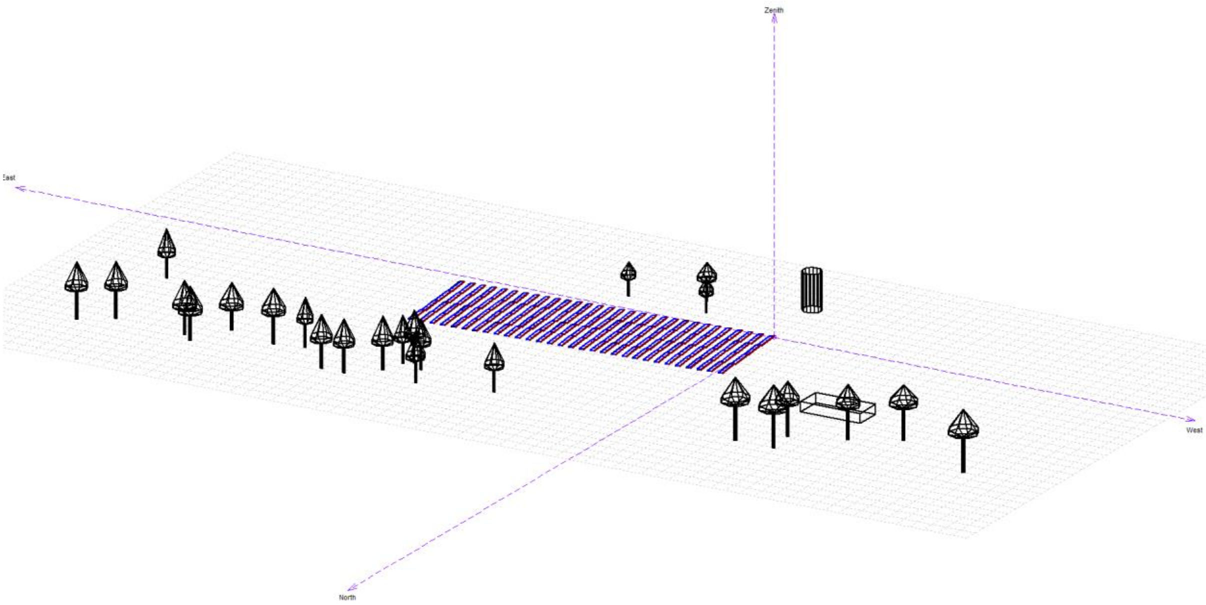

Panel (C). DAT array

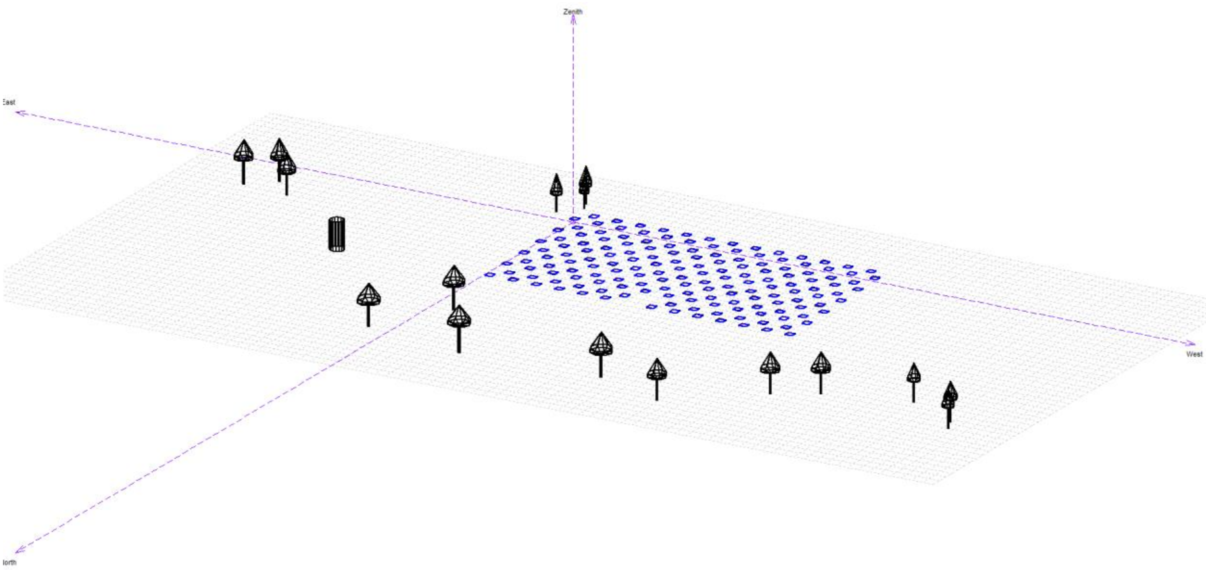

During a simulation, the shading factors are calculated at each hour, and applied differently on the beam, diffuse and albedo components (PVsyst, 2016c). In the case of the beam component, a shading factor is calculated as the shaded fraction of the PV field with respect to the full sensitive area. This shading factor is calculated for the effective direction of the sun at the middle of each hourly time-step (PVsyst, 2016d).

In the case of the diffuse component, the reduction in diffuse POA irradiance is modelled by a single sky diffuse loss percentage. In calculating this, an isotropic diffuse radiation model is assumed in which diffuse radiation is assumed to be uniformly distributed across the sky. This shading factor is calculated by integrating the shading factor over all the sky directions seen by the collectors between the collector plane and the horizontal plane. Because this component does not depend upon the position of the sun, but only on the system geometry, it is constant over the whole year (PVsyst, 2016d).

The calculation of both diffuse and albedo loss factors is more complicated when applied to tracking systems. For tracking systems, a whole set of shading tables needs to be calculated for each tracker position and the diffuse loss calculated by integrating over each of those tables. However, this procedure would be very expensive to implement in terms of the computation time. In PVsyst, a simple approximation method is implemented. Specifically, a significant tracker is chosen by the software in the middle of the system and the shading table is evaluated for this tracker using neighbouring trackers and ignoring other potential sources of shading. This translates into the evaluation of shading factors for approximately 12 tracker positions in a DAT system and approximately eight trackers in a SAT system (PVsyst, 2016e).

In relation to the albedo component, we can define this as the component seen by the collectors only if no close obstacle is present at the level of the ground. For near-object shading, the albedo component is calculated as the shading factor at zero height by integrating on the portion of the sphere under the horizon between the horizontal plane and the plane of the collectors. As with the diffuse component, this integral is not dependent on the sun's position and is therefore constant over the whole year (PVsyst, 2016d). However, a similar complication arises in the case of evaluating albedo loss for tracking systems as was mentioned in relation to the diffuse component. As such, albedo losses for tracking systems are also evaluated in the same heuristic way as mentioned above for diffuse losses (PVsyst, 2016e).

In PVsyst, self-shading effects of the three representative arrays are also accommodated in the modelling. Self-shading refers to visible shades drawn on parts of the representative arrays from nearby rows of modules in the same array. Key determinants of self-shading impacts are the tilt angle of modules and row spacing of modules. Both higher tilt angles and smaller distances between neighbouring sets of rows will typically cast larger shadings on nearby rows of modules in the same array.

The design settings adopted for self-shading analysis are listed in Table 3. For the representative FT array, the basic design structure encapsulated ten rows of modules, with each row containing four modules stacked vertically on top of each other in landscape orientation. The number of modules along each row was 180. The North-South (N-S) row spacing between each row was 4.27 metres.

In the case of the SAT array, there are 30 rows with 4 modules stacked vertically on top of each other in landscape orientation. The number of modules along the bottom of each row is 60. The East-West (E-W) row spacing between each row is 7.31 metres.

Some license had to be taken in order to model the DAT array in PVsyst. The actual DAT module layout at GSRF contains a mixture of modules in portrait and landscape orientation on each individual DAT tracker. Each DAT tracker contains 45 modules with 3 strings in parallel containing 15 modules each. PYSyst, however, cannot accommodate module layout containing a mixture of different module orientations. It also requires that the string layout be square or rectangular in construction. Given the need to have 45 modules in three strings on each individual DAT tracker, this severely restricts the module layout that can be employed in PVsyst.

In the simulations performed for this paper, we employed a rectangular structure containing nine rows of modules in landscape orientation. This means that there are five modules column-wise for each row on each individual DAT tracker, with three rows of five modules comprising an individual string. These dimensions produce a DAT array that is higher than the layout at GSRF and also smaller in width. As such, the DAT modelling is clearly an approximation that most likely understates the true impacts of self-shading given the actual longer width dimensions at GSRF. However, it is likely to give the closest approximation available given the constraints imposed on the layout of each DAT tracker by the PVsyst software. It is also likely to provide a more accurate estimate of PV Yield than would be forthcoming if self-shading impacts were ignored.

In Table 3, the results listed for the DAT array represent the results for an individual tracker. That is, there are: (1) 45 modules; (2) tracker height and width are is 5.58 and 6.1 metres; (3) N-S row spacing of 20.62 metres; and (4) E-W row spacing of 21.42 metres.

Because the modules used in the three representative arrays are thin film First Solar FS-395 PLUS modules, we employ the linear shading option in PVsyst to model near-object and self-shading effects of all three representative arrays. This option is for specially-designed thin film modules with cells and bypass diodes wired in such a way that the modules output varies linearly with shaded area of the module.

Table 3. Self-shading Design Settings Used In PVsyst Modelling

Design Feature	FT array	SAT array	DAT array
PVsyst PV Field Type	Fixed Tilted Plane	Tracking tilted or horiz. N-S axis	Tracking two axis
PVsyst 3d Shading PV Field Object	Shed Field	Tracking Field	Tracking Field
Number of modules along the side of row	4	4	9
Number of modules along the bottom of row	180	60	5
Number of rows or trackers (for DAT)	10	30	160
Shading algorithm	Thin film (linear)	Thin film (linear)	Thin film (linear)
Module orientation	Landscape	Landscape	Landscape
Length of side (in metres)	2.48	2.48	5.58
N-S Row spacing (in metres)	4.27	N.A.	20.62
E-W Row spacing (in metres)	N.A.	7.31	21.42

Iso-shading curves (PVsyst, 2016g) for the direct beam component of near-object and self-shading effects for each representative array are documented in Figure 4, Panels (A)-(C). Note in these figures that the path of the sun is defined according to azimuth angle (horizontal axis), sun elevation (vertical axis) as well as by time and date. This path is depicted by the yellow surface in each panel of Figure 4. These panels also contain iso-lines denoting 1, 5, 10, 20 and 40 per cent shading losses according to time and date generated by PVsyst. The actual dates included in the panels for which the shading losses are depicted correspond to 19 January, 21 February, 20 March, 20 April, 22 May, 22 June, 23 July, 23 August, 23 September, 23 October, 22 November and 22 December. Thus, all these dates fall during the second half of each respective month.

Figure 4. Iso-Solar Graphs of Direct Beam Shading Factors (percentage)

Panel (A). FT array

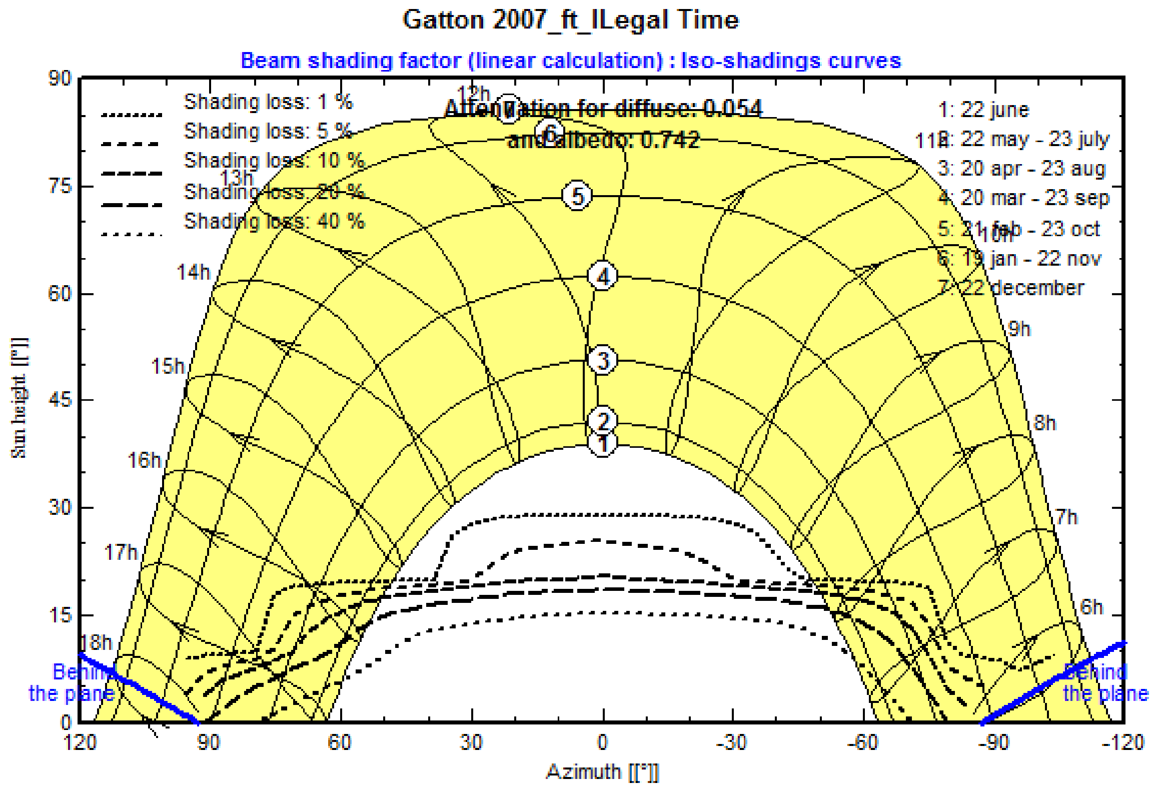

Panel (B). SAT array

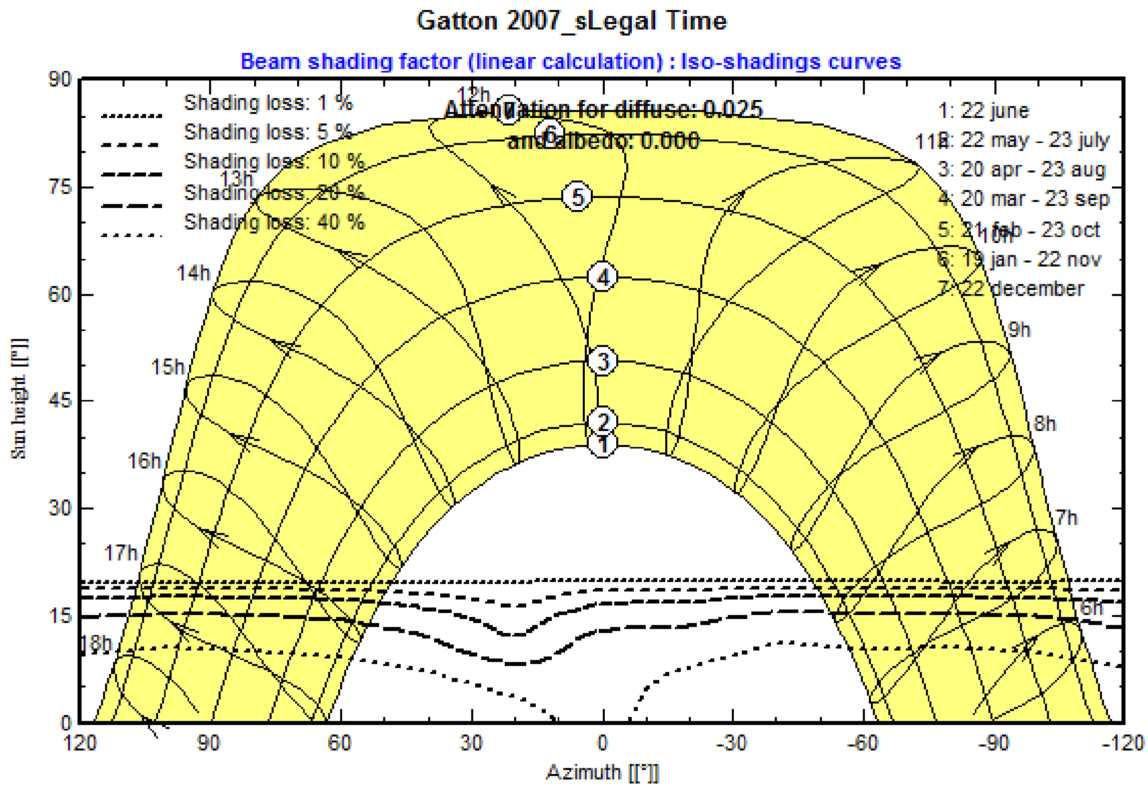

Panel (C). DAT array

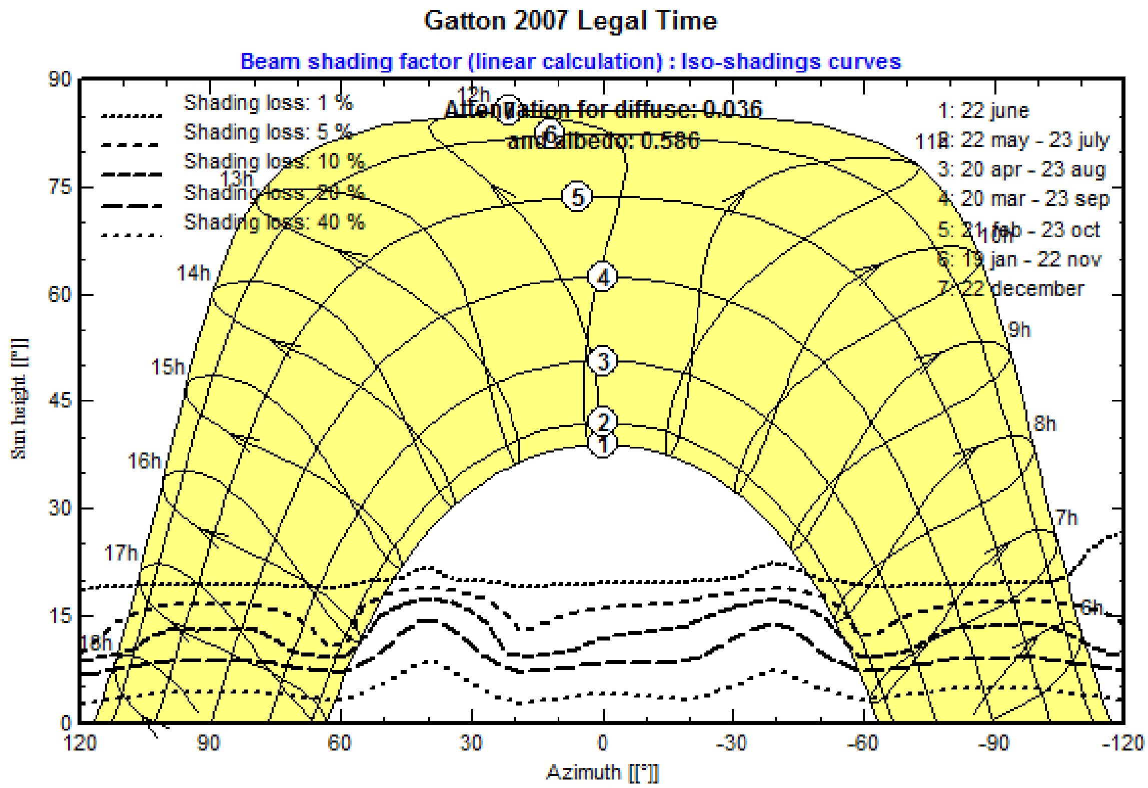

It is apparent from Figure 4 that the iso-lines for the FT array (Panel A) differ qualitatively from those associated with the SAT and DAT arrays. First, the concept of 'behind the plane' only applies to the FT array. The sun is active on the surface of the two tracking arrays because of their ability to track the sun's azimuth angle. Second, the path of the iso-shading loss lines in the case of the SAT and DAT arrays [in Panels (B) and (C)] appear quite horizontal during the early morning and late afternoon time frames – e.g. between (+/-) 50 and (+/-) 115 degrees azimuth. In Panel (A) for the FT array, these iso-shading lines are more downward sloping as the magnitude of the azimuth angle increases within the(+/-) 50 and (+/-) 115 degree band and clearly approach the behind the plane barrier especially in winter.

The iso-lines depicting 1, 5, 10, 20 and 40 per cent shading losses in Figure 4 have been used to construct a representation of the shading losses by time and month and are documented in Table 4, Panels (A), (B) and (C) for the FT, SAT and DAT arrays. Values of 100 denote complete shading. Values of zero indicate no shading impacts and partial shading effects are represented by values between zero and 100, with larger impacts associated with higher magnitude values. Note that the lower and upper limits of the shading losses reported in Table 4 correspond to the discrete set of lower and upper bound shading losses presented in Figure 4. That is, losses lying between 1 per cent and 40 per cent. Moreover, in Table 4 we present the minimum shading losses appearing in each hour within the band of one per cent to 40 per cent. This choice of minimum gives an indication of the maximum hourly extent of the shading losses by hour and by date. This follows because the lower shading losses would be the last shading effects to disappear within each hour in the morning and the earliest shading effects to appear in the afternoon.

In general, the DAT array (Panel C) has the lowest shading impacts in the early morning and later evening hours when compared to the shading effects on both the FT and SAT arrays. The FT array has the next lowest shading impacts with the SAT array experiencing marginally higher shading effects. This latter outcome is likely to be associated with the location of the trees and buildings in Panel (B) of Figure 3 lying to the north-east and north-west of the SAT array. These sets of trees are likely to be in position to partially interdict sunlight in the early morning and later evening hours, especially in winter when the sun is lower on the horizon. More generally, the representative FT and SAT array's experience very little or no direct beam shading over the period 8.00 am to 3.00 pm. In contrast, the representative DAT array experiences very little or no direct beam shading over a slightly broader time horizon of 7.00 am to 4.00 pm. However, there is some indication of slightly higher shading rates during winter in the range of 10 per cent at both 7.00 am and 4.00 pm for the DAT array.

Table 4. Direct Beam Shading Factors (Percentage): Minimum shading losses within each hour

Panel (A). FT array

Month	5:00 AM	6:00 AM	7:00 AM	8:00 AM	9:00 AM	10:00 AM	11:00 AM	12:00 PM	1:00 PM	2:00 PM	3:00 PM	4:00 PM	5:00 PM	6:00 PM
JAN	100	0.0	0.0	0.0	0.0	0.0	0.0	0.0	0.0	0.0	0.0	0.0	0.0	1.0
FEB	100	1.0	0.0	0.0	0.0	0.0	0.0	0.0	0.0	0.0	0.0	0.0	1.0	100
MAR	100	1.0	0.0	0.0	0.0	0.0	0.0	0.0	0.0	0.0	0.0	0.0	1.0	100
APR	100	20.0	1.0	0.0	0.0	0.0	0.0	0.0	0.0	0.0	1.0	5.0	40.0	100
MAY	100	100	20.0	1.0	0.0	0.0	0.0	0.0	0.0	0.0	1.0	20.0	100	100
JUN	100	100	40.0	1.0	0.0	0.0	0.0	0.0	0.0	0.0	1.0	40.0	100	100
JUL	100	100	20.0	1.0	0.0	0.0	0.0	0.0	0.0	0.0	1.0	20.0	100	100
AUG	100	20.0	1.0	0.0	0.0	0.0	0.0	0.0	0.0	0.0	1.0	5.0	40.0	100
SEP	100	1.0	0.0	0.0	0.0	0.0	0.0	0.0	0.0	0.0	0.0	0.0	1.0	100
OCT	100	1.0	0.0	0.0	0.0	0.0	0.0	0.0	0.0	0.0	0.0	0.0	1.0	100
NOV	100	0.0	0.0	0.0	0.0	0.0	0.0	0.0	0.0	0.0	0.0	0.0	0.0	1.0
DEC	100	0.0	0.0	0.0	0.0	0.0	0.0	0.0	0.0	0.0	0.0	0.0	0.0	1.0

Panel (B). SAT array

Month	5:00 AM	6:00 AM	7:00 AM	8:00 AM	9:00 AM	10:00 AM	11:00 AM	12:00 PM	1:00 PM	2:00 PM	3:00 PM	4:00 PM	5:00 PM	6:00 PM
JAN	100	1.0	0.0	0.0	0.0	0.0	0.0	0.0	0.0	0.0	0.0	1.0	5.0	100
FEB	100	20.0	1.0	0.0	0.0	0.0	0.0	0.0	0.0	0.0	0.0	1.0	10.0	100
MAR	100	40.0	1.0	0.0	0.0	0.0	0.0	0.0	0.0	0.0	0.0	1.0	40.0	100
APR	100	100	1.0	0.0	0.0	0.0	0.0	0.0	0.0	0.0	1.0	5.0	100	100
MAY	100	100	40.0	1.0	0.0	0.0	0.0	0.0	0.0	0.0	1.0	20.0	100	100
JUN	100	100	40.0	1.0	0.0	0.0	0.0	0.0	0.0	0.0	1.0	40.0	100	100
JUL	100	100	40.0	1.0	0.0	0.0	0.0	0.0	0.0	0.0	1.0	20.0	100	100
AUG	100	100	1.0	0.0	0.0	0.0	0.0	0.0	0.0	0.0	1.0	5.0	100	100
SEP	100	40.0	1.0	0.0	0.0	0.0	0.0	0.0	0.0	0.0	0.0	1.0	40.0	100
OCT	100	20.0	1.0	0.0	0.0	0.0	0.0	0.0	0.0	0.0	0.0	1.0	10.0	100
NOV	100	1.0	0.0	0.0	0.0	0.0	0.0	0.0	0.0	0.0	0.0	1.0	5.0	100
DEC	40.0	1.0	0.0	0.0	0.0	0.0	0.0	0.0	0.0	0.0	0.0	0.0	1.0	100

Panel (C). DAT array

Month	5:00 AM	6:00 AM	7:00 AM	8:00 AM	9:00 AM	10:00 AM	11:00 AM	12:00 PM	1:00 PM	2:00 PM	3:00 PM	4:00 PM	5:00 PM	6:00 PM
JAN	20.0	1.0	0.0	0.0	0.0	0.0	0.0	0.0	0.0	0.0	0.0	0.0	1.0	40.0
FEB	40.0	5.0	1.0	0.0	0.0	0.0	0.0	0.0	0.0	0.0	0.0	1.0	5.0	40.0
MAR	100	10.0	1.0	0.0	0.0	0.0	0.0	0.0	0.0	0.0	0.0	1.0	20.0	100
APR	100	20.0	1.0	0.0	0.0	0.0	0.0	0.0	0.0	0.0	1.0	5.0	40.0	100
MAY	100	40.0	5.0	1.0	0.0	0.0	0.0	0.0	0.0	0.0	1.0	10.0	100	100
JUN	100	100	10.0	1.0	0.0	0.0	0.0	0.0	0.0	0.0	1.0	10.0	100	100
JUL	100	40.0	5.0	1.0	0.0	0.0	0.0	0.0	0.0	0.0	1.0	10.0	100	100
AUG	100	20.0	1.0	0.0	0.0	0.0	0.0	0.0	0.0	0.0	1.0	5.0	40.0	100
SEP	100	10.0	1.0	0.0	0.0	0.0	0.0	0.0	0.0	0.0	0.0	1.0	20.0	100
OCT	40.0	5.0	1.0	0.0	0.0	0.0	0.0	0.0	0.0	0.0	0.0	1.0	5.0	40.0
NOV	20.0	1.0	0.0	0.0	0.0	0.0	0.0	0.0	0.0	0.0	0.0	0.0	1.0	40.0
DEC	10.0	1.0	0.0	0.0	0.0	0.0	0.0	0.0	0.0	0.0	0.0	0.0	1.0	10.0

The constant sky diffuse and albedo shading losses for the three representative arrays are listed in Table 5. These values were calculated by PVsyst to be 0.054, 0.025 and 0.036 for the representative FT, SAT and DAT arrays. Similarly, the albedo components were calculated to be 0.742, 0.000 and 0.586. Both diffuse and albedo loss factors are lower for the tracking systems when compared with the FT system.

Table 5. Diffuse and Albedo Shading Factors (Proportion)

Array	Diffuse	Albedo
FT	0.054	0.742
SAT	0.025	0.000
DAT	0.036	0.586

(3.1.5) DC and AC electrical losses

We have also adopted the following values for derating DC array output associated with DC electrical losses of between 3.56 and 3.99 per cent, depending upon the array technology, and AC electrical losses of 2.2 per cent. Details of specific settings are listed in Appendix A, Panel (C). It should be recalled that the DC 'Mismatch' and 'Nameplate' loss factors were partially reduced to ensure that net losses were zero when modification were made to ensure that the augmented soiling loss factors adjusted for local spectrum were non-negative. More information about typical loss factor settings for Solar PV simulations can be found in Thevenard et al (2010), Tapia Hinojosa (2014) and ARUP (2015, Section 4.2).

Other modelling assumptions utilised in the simulations are:

- No electrical shadings effects are applied because the First Solar modules are orientated correctly in landscape orientation to eliminate these effects.
- Power sorting tolerance adjustments were not considered.
- Continuous daytime auxiliary loss of 1950W and overnight consumption of 100W was assumed. The total annual self-consumption was calculated based on 8 hours of operation during the day at the maximum self-consumption rate of 1950W and 16 hours of night time self-consumption at 100W, which equates to 6.28MWh/year per inverter. These estimates are upper range estimates of auxiliary losses.
- Plant and grid availability and grid curtailment was not considered.

(3.2) Assessment of Simulated Annual Production Levels

Once all the required inputs have been made available to PVsyst, simulations can be performed to assess the production outcomes of each representative solar PV technology. The production results from the modelling are reported in Table 6, Panels (A)-(C) for the low, medium and high soiling scenarios.

Given the focus of economic viability studies on revenue earnt from electricity supplied directly to the grid, we calculate annual electricity production but exclude any electricity used internally by the system at night. Specifically, we calculate the annual production levels by aggregating the hourly system output after zeroing out any negative hourly production entries associated with internal night-time consumption of electricity by the system. Thus, this production concept reflects an energy sent-out production concept, that is, the electricity exported to the grid during the day that is available to earn revenue by servicing demand.

Two particular revenue streams are envisaged. The first is revenue attributed to the solar array associated with reduction in grid off-take of electricity which is subsequently replaced by electricity produced by the solar array itself. The second revenue stream is revenue from the sale of Large-scale Generation Certificates (LGC) through the production of eligible renewable energy under the Australian Government's Large-scale Renewable Energy Target (LRET) scheme (CER, 2016).

The second last row of each panel of Table 6 contains the average production levels whilst the last row in each panel contains aggregate total production calculated from the annual results listed above for the period 2007–2015. Assessment of all panels of Table 6 indicates considerable year-on-year variation. Of particular note is the sizable reduction in 2010, in relative terms, corresponding to the onset of a severe La Nina, especially over the second half of 2010. Relatively higher production totals were also recorded in 2007 and over 2012–2014 when coming out of relatively weak El Nino and sustained La Nina patterns, respectively. The production levels are largest in magnitude in 2014, reflecting the onset of ENSO neutral conditions but with a strongly emerging El Nino bias. Interesting, however, is the reduction in annual production arising in 2015, relative to 2013–2014, accompanying the formal move to severe El Nino conditions in 2015.

Table 6. Production Totals by Array Type and Soiling Scenario

Panel (A). Low soiling

Year	FT	SAT	DAT_CMD
2007	1147.2	1347.6	1571.4
2008	1124.5	1331.0	1552.8
2009	1132.0	1329.8	1561.8
2010	1016.6	1175.9	1367.2
2011	1093.9	1272.1	1476.3
2012	1156.1	1368.2	1577.7
2013	1175.1	1410.7	1633.4
2014	1204.8	1421.9	1655.9
2015	1147.9	1345.8	1529.5
Average	1133.1	1333.7	1547.3
Total	10198.1	12003.0	13925.9

Panel (B). Medium soiling

Year	FT	SAT	DAT_CMD
2007	1130.2	1328.7	1548.8
2008	1107.7	1312.3	1530.7
2009	1114.2	1310.0	1538.1
2010	1001.6	1159.5	1347.9
2011	1077.5	1254.1	1454.9
2012	1139.2	1349.5	1555.6
2013	1157.7	1391.2	1610.4
2014	1187.0	1402.0	1632.2
2015	1131.5	1327.7	1508.6
Average	1116.3	1315.0	1525.2
Total	10046.6	11834.9	13727.2

Panel (C). High soiling

Year	FT	SAT	DAT_CMD
2007	1102.2	1296.9	1511.8
2008	1079.7	1280.4	1493.7
2009	1085.3	1277.0	1499.5
2010	976.7	1132.0	1315.9
2011	1050.6	1224.1	1420.0
2012	1111.0	1317.6	1518.6
2013	1128.7	1357.9	1571.8
2014	1157.5	1368.6	1593.1
2015	1104.0	1297.0	1473.6
Average	1088.4	1283.5	1488.7
Total	9795.7	11551.4	13398.1

The system-wide impacts of soiling can also be discerned from Table 6. Under low soiling, average annual production levels of 1133.1, 1333.7 and 1547.3 MWh are reported in Panel (A) for the representative FT, SAT and DAT arrays. Similarly, total production for the period 2007–2015 of 10198.1, 12003.0 and 13925.9 MWh was also recorded. Comparison of these results with the equivalent values associated with medium and high soiling point to reductions in both production measures for all three representative arrays. Furthermore, the rate of reduction in average annual and total production relative to the low soiling increases with the level of module soiling.

Specifically, for the representative FT array, average annual production was reduced by 1.48 and 3.94 per cent, relative to the low soiling scenario's average annual production level cited above. For the SAT array, the equivalent reduction in annual average production was 1.40 and 3.76 per cent, respectively. In the case of the DAT array, the reduction was 1.43 and 3.79 per cent. Using total production instead of average annual production produces similar percentage sized reductions. Moreover, comparing the percentage reduction in both production measures for the high soiling scenario relative to the medium soiling scenario, the percentage reductions are in the order of 2.50, 2.40 and 2.39 per cent, respectively, for the FT, SAT and DAT arrays.

These results indicate that the output of the representative FT array is more adversely affected by increased module soiling relative to the solar PV yields of the SAT and DAT arrays. This is seen in the higher percentage reduction rates associated with the FT array when compared with the other two representative arrays. The results are somewhat mixed for the SAT and DAT arrays. When compared against the low soiling production results, the SAT array has slightly lower percentage reduction rates when compared with the DAT array. However, when comparing the high soiling production outcomes against the medium soiling production results, the DAT array now has marginally lower percentage reduction rates. However, in overall terms, solar tracking ability seems to help partially insulate against the adverse impacts of module soiling on solar PV yield.

Recall that a key metric often sought when comparing the performance of solar PV tracking systems relative to a benchmark FT system is the extent to which output of the tracking systems exceeds that of the benchmark FT system. These results are reported in Panels (A)-(C) of Table 7 in relation to the annual production data reported in Table 6 for the three soiling scenarios being considered. The data in Table 7 documents the percentage increase in output of the SAT and DAT trackers relative to the output of the FT array. As such, in Table 7, Panel (A) for year 2007, the values of 17.5 and 37.0 indicate that the output of the SAT and DAT arrays recorded in Table 6, Panel (A) for year 2007 (e.g. 1347.6 and 1571.4 MWh's) are 17.5 and 37.0 per cent higher than the corresponding output of the FT array (1147.2 MWh). Note that for the SAT technology, the percentages reported in the second column of Table 7 are calculated for each year as:

$$Percentage_{SAT} = \left[\frac{\left(\Pr od_{SAT} - \Pr od_{FT}\right)}{\Pr od_{FT}} \right] \times 100 \qquad (1)$$

where $'\Pr od_{FT}'$ and $'\Pr od_{SAT}'$ refer to the yearly annual production data reported in Table 6 for the FT and SAT arrays. The percentages for the DAT technology listed in Column 3 of Table 7 can also be calculated in a similar manner after replacing the 'SAT' subscripts in (1) with 'DAT' subscripts.

Examination of Table 7 once again indicates year-on-year variation in the percentage figures and also by soiling scenario. For the SAT array, the gains in production are bounded between 15.7 and 20.0 per cent for low soiling [Panel (A)], between 15.8 and 20.2 per cent for medium soiling [Panel (B)], and between 15.9 and 20.3 per cent for the high soiling scenario [Panel (C)]. The average percentage increase in solar PV yield for this array type relative to the FT array for the period 2007–2015 are listed in the last row of each panel in

Table 7 and are 17.7, 17.8 and 17.9 per cent, respectively. Thus, the average results listed in Table 7 for the representative SAT array generally increases with soiling indicating that the SAT array tracking behaviour improves the solar PV yield relative to the benchmark FT array as the level of module soiling increases.

In the case of the DAT array, the results in Table 7 are bounded between 33.2 and 39.0 per cent for low soiling [Panel (A)], between 33.3 and 39.1 per cent for medium soiling [Panel (B)], and between 33.5 and 39.3 per cent for the high soiling scenario [Panel (C)]. The average percentage increase in solar PV yield for this array relative to the FT array for the period 2007–2015 are 36.5, 36.6 and 36.7 per cent, respectively. Once again, the increase in the average value with soiling scenario indicates that the DAT array's tracking behaviour improves the solar PV yield relative to the FT array as the level of soiling increases. Furthermore, relative to the output of the benchmark FT array, the higher absolute percentage values for the DAT array in Table7 also clearly underpin the greater production of electricity coming from the DAT array when compared with the SAT array.

Table 7. Percentage Change in Production for SAT and DAT Tracking Systems Relative to FT System by Soiling Scenario

Panel (A). Low soiling

Year	SAT	DAT
2007	17.5	37.0
2008	18.4	38.1
2009	17.5	38.0
2010	15.7	34.5
2011	16.3	35.0
2012	18.4	36.5
2013	20.0	39.0
2014	18.0	37.4
2015	17.2	33.2
Average	17.7	36.5

Panel (B). Medium soiling

Year	SAT	DAT
2007	17.6	37.0
2008	18.5	38.2
2009	17.6	38.0
2010	15.8	34.6
2011	16.4	35.0
2012	18.5	36.6
2013	20.2	39.1
2014	18.1	37.5
2015	17.3	33.3
Average	17.8	36.6

Panel (C). High soiling

Year	SAT	DAT
2007	17.7	37.2
2008	18.6	38.3
2009	17.7	38.2
2010	15.9	34.7
2011	16.5	35.2
2012	18.6	36.7
2013	20.3	39.3
2014	18.2	37.6
2015	17.5	33.5
Average	17.9	36.7

The average results cited in the last row of each panel of Table 7 are broadly consistent with findings in the literature. Manufacturer's claims often assert increases of up to 30% for single axis tracking systems and up to 40% for dual axis tracking systems (Sabry and Raichle, 2013). Results cited in Koussa *et al.* (2011) point to gains for SAT systems of between 16 to 20 per cent for regions with poor irradiance and 28 to 36 per cent for regions with abundant irradiance. In the case of DAT systems, production gains fell in the range 29.3 to 41 per cent. Robinson and Raichle (2012) cite values from studies of SAT systems of between 29.3% and 42% and between 29.2% and 54%, depending upon the geographic location and climatic conditions underpinning the studies. Mousazadeh et al. (2009, p. 1802) cite general evidence pointing to gains of between 30% and 40% in good areas (and conditions) and in the low 20% range in poor conditions such as cloudy and hazy locations. More generally, in their detailed survey of efficiency gains reported in the literature relating to active solar tracking systems, they report evidence pointing to gains in production in the range of 20% to 30% for single axis tracking systems and between 30% and 45% for two axis tracking systems (Mousazadeh et al., 2009, pp. 1807–1810).

Using the above results as a broad guide, the average results reported in Table 7 would seem to be within the mid-range of these estimates cited in the broader literature for the DAT array and towards the lower end of the range of estimates for the SAT system.

(3.3) Assessment of Simulated Annual Capacity Factor Outcomes

Once the annual production outcomes have been calculated for the three representative arrays at GSRF, it is a simple process to calculate the annual capacity factor (ACF) outcomes of each representative system. The ACF is calculated by the following equation:

$$ACF = \left[\frac{Annual\_\mathrm{Pr}\,od}{\left(8760 \times System\_Capacity\right)} \right], \tag{2}$$

where ‘8760’ represents the number of hours in a year assuming a 365 day year.[2] The ACF results for the three representative arrays are reported in Table 8, Panels (A)–(C) for the low, medium and high soiling scenarios. Note that the production concept [e.g. variable $'Annual\_\mathrm{Pr}\,od'$ in (2)] is based on the annual production totals for each soiling scenario reported in Table 6 and variable $'System\_Capacity'$ corresponds to the 630 kW capacity limit of each of the inverters.

[2] Note that for leap years (e.g. 2008 and 2012), we use 8784 hours in a year in (2) instead of 8760.

Table 8. Energy Sent-out ACF by Array Type by Soiling Scenario[3]

Panel (A). Low soiling

Year	FT	SAT	DAT
2007	20.8	24.4	28.5
2008	20.3	24.0	28.1
2009	20.5	24.1	28.3
2010	18.4	21.3	24.8
2011	19.8	23.0	26.7
2012	20.9	24.7	28.5
2013	21.3	25.6	29.6
2014	21.8	25.8	30.0
2015	20.8	24.4	27.7
Annualised Average	20.5	24.2	28.0

Panel (B). Medium soiling

Year	FT	SAT	DAT
2007	20.5	24.1	28.1
2008	20.0	23.8	27.7
2009	20.2	23.7	27.9
2010	18.1	21.0	24.4
2011	19.5	22.7	26.4
2012	20.6	24.4	28.1
2013	21.0	25.2	29.2
2014	21.5	25.4	29.6
2015	20.5	24.1	27.3
Annualised Average	20.2	23.8	27.6

[3] Because of satellite problems, data was missing from the BOM's hourly solar irradiance dataset for: (1) year 2008, 1 –17 March and 10–13 of April, representing 192 hours of missing data; and (2) year 2009, 17–18 February, 12 and 16–27 of November, representing 360 hours of missing data. Thus, the ACF's reported in Table 8 for 2008 and 2009 will under-state the true ACF's for these two particular years.

Panel (C). High soiling

Year	FT	SAT	DAT
2007	20.0	23.5	27.4
2008	19.5	23.1	27.0
2009	19.7	23.1	27.2
2010	17.7	20.5	23.8
2011	19.0	22.2	25.7
2012	20.1	23.8	27.4
2013	20.4	24.6	28.5
2014	21.0	24.8	28.9
2015	20.0	23.5	26.7
Annualised Average	19.7	23.3	27.0

Inspection of Table 8 points to considerable variation in the ACF's on a year-by-year basis, as was also observed with the production totals listed in Table 6. Specifically, and mirroring the production outcomes, the lowest ACF's were recorded in year 2010 and the highest were recorded in 2014. For the low, medium and high soiling scenarios, the ACF results for the benchmark FT technology fall within the range 18.4 to 21.8 per cent, 18.1 to 21.5 per cent and 17.7 to 21.0 per cent. For the period 2007 to 2015, the average ACF values for the FT array were determined to be 20.5, 20.2 and 19.7 per cent for the low, medium and high soiling scenarios.

In the case of the SAT array, the equivalent ACF outcomes for each soiling scenario were in the range of 21.3 to 25.8 per cent, 21.0 to 25.4 per cent and 20.5 to 24.8 per cent, respectively, with average ACF outcomes being 24.2, 23.8 and 23.3 per cent. For the DAT array, the equivalent ACF outcomes were in the range of 24.8 to 30.0 per cent, 24.4 to 29.6 per cent and 23.8 to 28.9 per cent. The average ACF outcomes by soiling scenario for the DAT array were 28.0, 27.6 and 27.0 per cent.

It is apparent from these results that for all three representative arrays, the average ACF results and their range clearly diminish as the level of module soiling increases. Moreover, mirroring the production results examined in the previous section, the ACF outcomes are highest for the representative DAT array, in the range of 27.0 to 28.0 per cent in average terms, depending on module soiling. This is followed by the results for the SAT array which, in average terms, are in the range 23.3 to 24.2 per cent. Finally, the representative FT array clearly has the lowest results with average ACF results for the period 2007–2015 in the range of 19.7 to 20.5 per cent.

(4) Conclusions

Economic assessment of the viability of different types of solar PV tracking technologies centres on an assessment of whether the annual production of the different tracking technologies is increased enough relative to the benchmark FT system to compensate for the higher cost of installation and operation incurred by the tracking systems. To assess this, in the first instance, simulation modelling of the PV yield of the different solar PV systems needs to be performed. In this paper, we restricted attention to an assessment of the production results of three representative 630 kW FT, SAT and DAT arrays located at UQ Gatton Campus GSRF.

The PVsyst software was used to simulate electricity production from the three representative solar PV systems. Data relating to hourly solar irradiance data, weather data, and surface albedo data for Gatton was sourced from the BOM and NASA. Technical data relating to both module and inverter characteristics were contained in internal PVsyst product databases. Impacts associated with module soiling, near-object shading and self-shading were also accommodated in the modelling.

Three broad module soiling scenarios were incorporated in the modelling - low, medium and high module soiling. These soiling scenarios were linked to hypothesised cleansing effects associated with rainfall and were also augmented to account for energy gains and losses associated with divergence of local spectrum conditions from STC conditions. These low, medium and high augmented soiling losses produced average annualised soiling rates of 1.7, 3.2 and 5.7 per cent, respectively, albeit with much more variability arising on a month-by-month basis.

A key finding was that over the period 2007–2015, average increases in annual production of between 17.7 and 17.9 per cent and 36.5 and 36.7 per cent were obtained for the SAT and DAT tracking systems relative to the FT system, depending on module soiling rates. These results fell within the mid-range of estimates for the DAT array and towards the lower end range of estimates for the SAT array cited in the literature.

ACF results were also calculated. The FT array had the lowest recorded average ACF values over 2007–2015 in the range 19.7 to 20.5 per cent, depending on module soiling. The SAT array had the next lowest average ACF values between 23.3 to 24.2 per cent, again depending upon module soiling rates. The highest ACF outcomes were recorded by the DAT array with average ACF results in the range of 27.0 to 28.0 per cent.

Another key finding was that the output of the representative FT array is more adversely affected by increased module soiling relative to the solar PV yields of the SAT and DAT arrays. This suggested that solar tracking ability can help partially insulate solar PV yield against the adverse impacts of module soiling. Future research will compare these predictions to actual data obtained from the GSRF array.

References

ACT: Australian Capital Territory (2016) ‘: ACT Government, Environment and Planning Directorate, Environment, Large-scale Solar.’ Available at: http://www.environment.act.gov.au/energy/cleaner-energy/large-scale-solar.

AGL (2015) ‘Fact Sheet: Nyngan Solar Plant.’ Available at: https://www.agl.com.au/~/media/AGL/About%20AGL/Documents/How%20We%20Source%20Energy/Solar%20Community/Nyngan%20Solar%20Plant/Factsheets/2014/Nyngan%20Fact%20Sheet%20v7.pdf.

ARENA (2016) ‘Australian Government Australian Renewable Energy Agency.’ Available at: http://arena.gov.au/..

ARUP (2015) ‘Energy Yield Simulations, Module Performance Comparison for Four Solar PV Module Technologies.’ Arup (Pty) Ltd Consulting Engineers, Johannesburg, South Africa, May 2015. Available at: http://www.bizcommunity.com/f/1505/Module_Performance_Comparison_for_Four_Solar_PV_Module_Technologies_08-0....pdf.

Australian Government Clean Energy Regulator: CER (2016) ‘Large-scale Renewable Energy Target.’ Available at: http://www.cleanenergyregulator.gov.au/RET/About-the-Renewable-Energy-Target/How-the-scheme-works/Large-scale-Renewable-Energy-Target. Accessed 25-5-2016.

Bureau of Meteorology: BOM (2015) ‘Australian Hourly Solar Irradiance Gridded Data.’ Available at: http://www.bom.gov.au/climate/how/newproducts/IDCJAD0111.shtml.

CEFC (2016) ‘Clean Energy Finance Corporation.’ Available at: http://www.cleanenergyfinancecorp.com.au/.

First Solar (2015) ‘Module Characterisation: Energy Prediction Adjustment for Local Spectrum’. First Solar Document Number PD 5-423.

Green Energy Markets (2015) ‘Renewables target needs 3,800MW of large-scale renewables within 12 months.’ Available at: http://greenmarkets.com.au/news-events/renewables-target-needs-3800mw-of-large-scale-renewables-within-12-months.

Green Energy Markets (2016) ‘Insight: Renewable Energy Target won’t be met in 2018.’ Available at: http://greenmarkets.com.au/resources/insight-ret-wont-be-met-in-2018.

Kimber, A., Mitchell, L., Nogradi, S., and H. Wenger (2006),’ The effect of soiling on large grid-connected photovoltaic systems in California and the southwest region of the United States.*’ In Conference Record of the 2006 IEEE 4th World Conference on Photovoltaic Energy Conversion*, Waikoloa, HI, 2006. Available at: http://ieeexplore.ieee.org/stamp/stamp.jsp?tp=&arnumber=4060159.

M. Koussa, M., Cheknane, A., Hadji, S., Haddadi, M., and S. Noureddine (2011) 'Measured and modelled improvement in solar energy yield from flat plate photovoltaic systems utilizing different tracking systems and under a range of environmental conditions,' *Applied Energy*, 88, pp. 1756-1771.

Mermoud, A., and B. Wittmer (2014) 'PVsyst User's Manual: PVsyst6' Available at http://www.PVsyst.com/images/pdf/PVsyst_Tutorials.pdf.

Mousazadeh, H., Keyhani, A., Javadi, A., and H. Mobli (2009) 'A review of principle and sun-tracking methods for maximising solar systems output', *Renewable and Sustainable Energy Reviews*, 13, pp. 1800-1818.

NASA (2015) 'Albedo 16-Day L3 Global 0.05Deg CMG'. Available at: https://lpdaac.usgs.gov/dataset_discovery/modis/modis_products_table/mcd43c3.

PVsyst (2016a) 'PVsyst: Photovoltaic Software', Available at: http://www.pvsyst.com/en/.

PVsyst (2016b) 'Horizon - Far shadings', Available at: http://files.pvsyst.com/help/horizon.htm.

PVsyst (2016c) 'Shadings - General'. Available at: http://files.pvsyst.com/help/shadings_general.htm.

PVsyst (2016d) 'Shadings treatment of Beam, Diffuse and Albedo'. Available at: http://files.pvsyst.com/help/shading_treatment.htm.

PVsyst (2016e) ' How is calculated the Shading Loss on diffuse with tracking systems?'. Available at: http://forum.PVsyst.com/viewtopic.php?f=30&t=694.

PVsyst (2016f) ' Transposition model'. Available at: http://files.pvsyst.com/help/.

PVsyst (2016g) 'PVsyst Iso-shading Diagrams". Available at: http://files.pvsyst.com/help/near_shadings_isoshadings.htm.

RMI: Rocky Mountain Institute and Georgia Tech Research Institute (2014) 'Lessons From Australia: Reducing Solar PV Costs Through Installation Labour Efficiency.' Available at: http://www.rmi.org/Knowledge-Center/Library/2014-11_RMI-AustraliaSIMPLEBoSFinal.

Robinson, J.W., and B.W. Raichle (2012) 'Performance Comparison of Fixed, 1-, and 2-Axis Tracking Systems for Small Photovoltaic Systems with Measured Direct Beam Fraction.' Proceedings of 42nd ASES Annual Conference, Denver, Colorado, May 2012. Available at: http://ases.conference-services.net/resources/252/2859/pdf/SOLAR2012_0261_full%20paper.pdf.

Sabry, M. S., and B. W. Raichle (2013) 'Determining the Accuracy of Solar Trackers'. *Proceedings of 42nd ASES Annual Conference*, Baltimore, Maryland, April 2013. Available at: http://proceedings.ases.org/wp-content/uploads/2014/02/SOLAR2013_0075_final-paper.pdf.

Sallaberry, F., de Jalon, A.G., Torres, J-L., and R. Pujol-Nadal (2015) 'Optical losses due to tracking error estimation for a low concentrating solar collector.' *Energy Conservation and Management*, **92**, pp. 194-206.

Stafford, B., Davis, M., Chambers, J., Martinez, M., and D. Sanchez (2009) 'Tracker accuracy: field experience, analysis, and correlation with meteorological conditions.' Photovoltaic Specials Conference (PVSC), 34 IEEE, June 2009. Available at: http://ieeexplore.ieee.org/stamp/stamp.jsp?tp=&arnumber=5411362.

Tapia Hinojosa., M (2014) 'Evaluation of Performance Models against Actual Performance of Grid Connected PV Systems.'Master's Thesis, Institute of Physics, Carl von Ossietzky Universität Oldenburg. Available at: http://oops.uni-oldenburg.de/2433/7/Thesis_TapiaM.pdf.

Thevenard, D., Driesse, A., Turcotte, D., and Y. Poissant (2010) 'Uncertainty in Long-term Photovoltaic Yield Projections.' CanmetENERGY, Natural Resources Canada, March. Available at: https://www.nrcan.gc.ca/sites/www.nrcan.gc.ca/files/canmetenergy/files/pubs/2010-122.pdf.

UQ (2015a) 'UQ, First Solar to build world-leading research centre.' Available at: https://www.uq.edu.au/news/article/2013/10/uq-first-solar-build-world-leading-research-centre

UQ (2015b) 'Fixed Tilt Array.' Available at: https://www.uq.edu.au/solarenergy/pv-array/content/fixed-tilt-array.

UQ (2015c) 'Single Axis tracking Array.' Available at: https://www.uq.edu.au/solarenergy/pv-array/content/single-axis-tracking-array.

UQ (2015d) 'Dual Axis tracking Array.' Available at: https://www.uq.edu.au/solarenergy/pv-array/content/dual-axis-array.

Appendix A. PVsyst Design and Parameter Settings

Panel (A): Albedo Settings by Year and Month

Month	2007	2008	2009	2010	2011	2012	2013	2014	2015
Jan	0.16	0.16	0.16	0.16	0.16	0.16	0.14	0.14	0.14
Feb	0.16	0.16	0.16	0.16	0.16	0.16	0.14	0.14	0.14
Mar	0.14	0.14	0.14	0.14	0.14	0.14	0.14	0.14	0.14
Apr	0.14	0.14	0.14	0.14	0.14	0.14	0.14	0.14	0.14
May	0.14	0.14	0.14	0.14	0.14	0.14	0.14	0.14	0.14
Jun	0.14	0.14	0.14	0.14	0.14	0.14	0.14	0.14	0.14
Jul	0.14	0.14	0.14	0.14	0.14	0.14	0.14	0.14	0.14
Aug	0.14	0.14	0.14	0.14	0.14	0.14	0.14	0.14	0.14
Sep	0.14	0.14	0.15	0.14	0.14	0.15	0.15	0.15	0.15
Oct	0.14	0.14	0.15	0.14	0.14	0.15	0.15	0.15	0.15
Nov	0.14	0.14	0.15	0.14	0.14	0.15	0.15	0.15	0.15
Dec	0.16	0.16	0.16	0.16	0.16	0.14	0.14	0.14	0.16

Panel (B): System Design

Description	Value	Measurement Unit
Modules per string	15	NA
Strings in parallel	480	NA
Number of inverters	1	NA
Configuration at reference conditions		
Modules:		
Nameplate capacity	684.0	kWdc
Number of modules	7,200	NA
Total module area	5,184	m^2
Inverters:		
Nameplate capacity – on output	630.0	kWac

Panel (C): DC and AC Losses

Description	FT Value (%)	SAT Value (%)	DAT Value (%)
DC Array Losses			
Mismatch	1.1	1.1	1.1
Diodes and connections	0.0	0.0	0.0
DC wiring	1.5	1.5	1.5
DC tracking losses	0.0	0.45	0.42
Module quality	1.0	1.0	1.0
DC power optimisation	0.0	0.0	0.0
Total DC losses	3.56	3.99	3.96
AC System losses			
AC wiring	1.0	1.0	1.0
Transformer losses	1.2	1.2	1.2
Total AC Losses	2.2	2.2	2.2